Advances in Computational Design, *Vol. 5, No. 1 (2020) 13-34*
DOI: https://doi.org/10.12989/acd.2020.5.1.013

An innovative CAD-based simulation of ball-end milling in microscale

Dimitrios G. Vakondios[1a] and Panagiotis Kyratsis*[2]

[1]Department of Product & System Design Engineering, University of the Aegean, Syros Island GR84100, Greece
[2]Department of Industrial Design Engineering, University of Western Macedonia, GR50100 Kila Kozani, Greece

(Received May 4, 2019, Revised September 5, 2019, Accepted September 26, 2019)

Abstract. As small size and complex metal machining components demand increases, cutting processes in microscale become necessary. Ball-end milling is a commonly used finishing process, which nowadays can be applied in the microscale size. Surface quality and dimensional accuracy are two basic parameters that affect small size components in their assembly and functionality. Thus, good quality can be achieved by optimizing the cutting conditions of the procedure. This study presents a 3D simulation model of ball-end milling in microscale developed in a commercial CAD software and its optical and computing results. These carried out results are resumed to surface topomorphy, surface roughness, chip geometry and cutting forces calculations that arising during the cutting process. A great number of simulations were performed in a milling machine centre, applying the discretized kinematics of the procedure and the final results were compared with measurements of Al7075-T651 experiments.

Keywords: micro-ball-end milling; CAD-based simulation; surface topomorphy; surface roughness; chip formation; cutting forces

1. Introduction

Ball-end milling, as a finishing process, is widely adapted in machining a variety of complex parts in many fields i.e. aerospace and biomedical applications. Generally, the machining of free-form surfaces, along an axis, using a ball-end cutting tool is challenging process that requires a variety of parameters to be optimized. The main parameters in such process are: a) feedrate, b) axial depth of cut, c) radial depth of cut and d) inclination of cutting tool axis. Small size and complexity of metal machining components are the main reasons for implementing milling in microscale. Micro-ball-end milling can be defined by the use of ball-end milling tools less than one millimeter in diameter.

The work of Kuram and Ozcelik investigates the effects of spindle speed, feed per tooth and depth of cut on tool wear, force components and surface roughness during micro-milling of

*Corresponding author, Associate Professor, E-mail: pkyratsis@uowm.gr
[a] Ph.D., E-mail: dvakondios@hotmail.com

Copyright © 2020 Techno-Press, Ltd.

aluminium using Taguchi experimental design method. Cutting tools and workpiece surfaces were also examined via scanning electron microscope (SEM) so that understand micro-milling process (Kuram and Ozcelik 2013).

Xie *et al*. proposed a 5-axial micro-replication milling of microstructured freeform surface by a novel ball cutter, on which micro-cutting-edge array is patterned by a diamond wheel V-tip in micro-grinding. Authors state that it can efficiently and precisely machine arbitrary-curved microgroove and micro-pyramid arrays on aluminium alloy and die steel. The form errors reach 6.6 mm in 253.6 mm in microstructure depth and 1.6 mm with 50 mm in macro-freeform, respectively. The rake angle, however, was decreased so as to increase cutting temperature. Moreover, increasing wheel speed and decreasing feed speed decrease micro-form errors and surface roughness. The cross-spark-out cutting may deburr (Xie *et al*. 2015).

In the work of Vehmeyer *et al*. a complex problem of micro surface generation is considered. Based on a micro mechanistic surface model, a parameter identification to meet a required tribological behaviour according to a bearing ratio curve (Firestone-Abbott curve) has been performed. In this study solely secured process knowledge like trochoidal tool motion and the minimum chip thickness concept is applied. For the dynamic tool oscillation a bottom-up strategy is pursued, which is solely based on topographic measurement and parameter identification. Furthermore, it turned out that a material flow must be considered for milling with intensive ploughing. A warp of material and material accumulation is modeled by a scaling factor (Vehmeyer *et al*. 2015).

The local parallel sliced method was applied to model 3D chip geometry to calculate ploughing chip volume and cutting forces in micro 5-axis flat-end milling by Luo *et al*. To get the ploughing volume and cutting forces, the cutter is divided into many layers. Chip thickness is a very important parameter for chip volume calculation. It can be obtained by removing the tool a distance of feed per tooth. Ploughing and shearing volume are calculated by adding volumes of small pieces of parallelepipeds along radial and axial direction. 5-axis simulation of cutting forces and chip volume has been carried out for milling cases that tool orientation and depth of cut change continuously. To better understand the ploughing effect problems in micro machining and to increase cutting efficiency, different feed rate were simulated to reduce the ploughing volume. The simulation cases led to the conclusion that high feed rate can reduce ploughing effect. As the feed per tooth is smaller than the minimum chip thickness, only ploughing volume exists (Luo *et al*. 2016).

Vyboishchik investigated various strategies of the pre-final working passes in ball-end milling of three different types of the machined freeform surfaces (oblique, convex, concave) of three strategies – “along the trace”, “across the trace” and “at an angle to the trace” of the rough machining passes. Six different models representing the combination of the freeform surfaces and the trace shape of the topology of the surface before machining are offered. The calculated dependencies allow forecasting of cutting forces, and, hence, the predictability in obtaining the surface accuracy (Vyboishchik 2016).

The work of Cai *et al*. investigated the effects of machined surface roughness on micro-nozzle performance, through computational fluid dynamics (CFD) simulations and experiment. Firstly, both ball end mill and taper end mill were used in the finish micro-milling processes for micro nozzles where different surface quality were obtained. A residue surface model for micro-nozzle was proposed and used in CFD simulation. The simulation results show that the increase of roughness causes that the outlet velocity decreases, total pressure drops and boundary layer thickness increases. The roughness increasing also leads to the deterioration of thrust performance

of the micro nozzle. Secondly, a thrust measuring apparatus was designed and manufactured to evaluate the thrust performance of the machined micro nozzle. The thrust was measured at different inlet pressure for the machined micro-nozzles with different surface roughness. The measurement results indicate that the simulation results were consistent with the experiment. The nozzle with small roughness can achieve better thrust performance. Actual thrust fluctuation was caused by the incremental turbulent intensity with surface roughness (Cai *et al*. 2016).

Baburaj *et al*. attempted to study edge radius of ball end mill at normal and transverse planes on a virtual ball end mill generated using kinematic relations in CAD environment. In the presented study, non-destructive methods using confocal microscope and stereo microscope are used to measure edge radius. These measurements capture the edge radius on the transverse plane. For confirmation, the tool sectioned in the transverse plane by a low speed diamond saw is examined under scanning electron microscope and the radius is assessed using suitable software. Among the non-contact approaches proposed in this work, confocal method appeared to be more reliable considering the reproducibility aspect (Baburaj *et al*. 2017).

Chen *et al*. performed cutting surface quality analysis in micro ball end-milling of KDP crystal by considering size effect and minimum undeformed chip thickness. The undeformed chip thickness in micro ball end-milling is calculated and deduced. The size effect, ductile cutting and brittle cutting zones with size effect and ductile-brittle transition boundaries in micro ball end-milling of KDP crystal are studied carefully by comprehensive analysis of the cutting force, specific cutting force, chip morphology and surface quality, and the cutting parameter which could achieve the best surface quality was also received (Chen *et al*. 2017).

Zhang *et al*. presented a new CWE model during 5-axis ball-end milling process, considering the effects of tool orientation, cutter runout and actual tool motion process, which can reach a higher calculation accuracy compared with the previous one. Based on the new cutting force prediction model, the tool orientation (lead and tilt angles) optimization strategies with a flexible cutter and rigid workpiece for roughing and finishing operations are developed. The optimization methods are conducted successfully for plane, cylindrical and spherical surfaces (Zhang *et al*. 2017).

Chen *et al*. developed a surface generation model for micro-end milling, by considering minimum chip thickness and tool runout in the machining process. A numerical model based on the trajectory and cutter geometry of micro-end mills was established, which can be used to describe the generation of machined surface profile and to estimate the surface roughness during the micro-end milling process. The simulation results were verified by micro milling experiments (Chen *et al*. 2017).

Wojciechowski *et al*. focused on the evaluation of mechanical and technological aspects of the micro ball end milling of hardened TOOLOX 44 steel. The experiment includes the measurement of acceleration of vibrations during the micro milling tests with variable feed per tooth and tool's axis inclination angle values. The next step involved the analysis of dynamics and the prediction of micro ball end milling forces on the basis of mechanistic model considering run out, variable edge forces, and kinematics of low radial immersion milling with tool axis inclination. Subsequently, the optimization of the micro ball end milling process was conducted. The obtained optimal values of tool's axis inclination angle and feed per tooth are validated during the micro milling tests involving the measurements of machined surface roughness. Results indicated that micro ball end milling with the optimally selected tool's axis slope along the toolpath and feed per tooth affects the minimization of milling vibrations and improvement in surface finish (Wojciechowski *et al*. 2017).

Aurich *et al*. investigated the influence of the tilt angle of the spindle on the generated surface quality, by kinematic simulations and experiments. Single edge micro end mills with an effective milling cutter diameter of 50 μm are applied. Recommendations are given to enhance process stability and surface quality (Aurich *et al*. 2017).

Liu *et al*. aimed to investigate the influences of the milling mode on the surface integrity of KDP brittle crystal. All the milling modes were considered (pull-milling, push-milling, up-milling and down-milling) and corresponding cutting parameters selections were also examined. The results demonstrated that the pull-milling and down-milling are both conducive to ductile mode machining, while the push-milling and up-milling cause adverse impacts on the machined surface integrity. In addition, the optimal combination of cutting parameters were also recommended to guide the mitigation of micro-defects on the surface of KDP crystal by micro ball-end milling process (Liu *et al*. 2018).

Wojciechowski *et al*. presented an analysis of relations between the instantaneous tool displacements and surface roughness formed during ball end milling of surface with inclination towards the tool's axis. A novel experimental method for the estimation of ball end mill's working part vibrations, considering displacements correlated with the geometrical errors of tool-toolholder-spindle system and deflections caused by milling forces has been proposed. The experiments have been conducted on hard-to-cut low carbon hardened alloy steel. Milling tests involved the use of monolithic ball end mills varied in terms of overhang l values (Wojciechowski *et al*. 2018).

Pratap and Patra applied a high speed ball-end micromilling process for fabrication of micro-textured surfaces with different configurations such as parallel micro-dimple, staggered micro-dimple and micro grid, in order to enhance the wettability of Ti-6Al-4V. Advancing and receding angles of both untextured and micro-textured surfaces were measured using nano-scale ultrapure deionized water droplet (Pratap and Patra 2018).

Wojciechowski *et al*. developed a method for the minimization of cutting forces and vibrations during precise ball end milling of hardened 55NiCrMoV6 steel. The aim of his work concentrated on the optimal selection of surface inclination angle α and tool's overhang l, which enables the minimization of cutting forces and vibrations in order to improve the machined surface quality (Wojciechowski *et al*. 2017).

Wang *et al*. research was on the micro milling performance of cermet and coated WC micro-mills with a diameter of 0.5 mm in machining of TC4 alloy in terms of tool wear, micro milling forces, and surface quality (Wang *et al*. 2018).

Eifler *et al*. proposed a systematic investigation of various control data parameters in order to achieve a sound understanding of their influence on the micro-milled surface quality and of micro milling as a manufacturing technology for material measures (Eifler *et al*. 2018).

Baburaj *et al*. presented an attempt to study on the forces involved in micro ball end milling of free-form surface machining. The off-centre mode ball end milling is closer to practical conditions to study the forces in micro free-form surface than the inclined milling tests. An experimental investigation is conducted to identify the ball-tip rubbing zone prior to off-centre milling tests (Baburaj *et al*. 2018).

Chen *et al*. investigated the textured surface generation mechanism in vibration-assisted micro milling through modeling and experimental approaches. To decouple the effects of tool geometry and kinematics of vibration-assisted milling, a surface generation model based on homogenous matrices transformation is proposed. On this basis, series of simulations are performed to provide insights into the effects of various vibration parameters on the generation mechanism of typical

textured surfaces in 1D and 2D vibration-assisted milling (Chen *et al*. 2019).

Simulation models are widely utilized by researchers in manufacturing processes, due to their various advantages. At first, there is the flexibility of the simulation model itself that makes it useful and easy. The main contribution of this study is the development of a simulation model of ball-end milling in microscale for 3D objects. The proposed methodology calculates attributes as surface topomorphy, surface roughness, chip geometry and cutting forces in relatively short times. Simulations outcomes are compared with actual values originating from milling processes using a Deckel Maho DMU 50 eco milling machine, controlled by the Siemens control 810D.

2. Cad-based ball-end micro-milling simulation

2.1 CAD-based simulation in micro-milling

Simulation models constitute a useful tool, both in the industrial sector and in research. Currently, there is a need in high-precision products. Also, the evolution of computers has led to the development of software simulation programs that assist in the production process and simultaneously reduce production costs. In Micromachining and Manufacturing Modeling Laboratory (m3) TUC, a three-dimensional simulation code of milling operation in micro-scale was developed. Three-dimensional simulation of machining procedures offers an advantage over other algebraic simulations as the generated three-dimensional solid contains the whole entire information on the process of cutting. The study of simulations' solid results may lead to estimation of useful factors and new results.

In the present study, a CAD-based model named Ball 3D was developed to simulate the ball-end milling process in microscale. Ball 3D was developed and can be executed through the Autodesk Inventor ™ interface. As a CAD system, Inventor ™ is competent for both the design of three-dimensional workpiece and cutting tool solids and the assembly of these two main parts. Thus, simulation can be reached step by step, while process kinematics is defined. Output data of the model are the three-dimensional surface topomorphy and undeformed chips.

MATLAB interface was chosen for the representation of three roughness parameters and cutting forces of the process. In these independent programs, numerical data that come of the geometry analysis of CAD model are graphically projected and values of both roughness parameters and cutting forces can be calculated.

Figure 1 presents the data flowchart of the designed 3D CAD-based simulation model.

2.2 Micromilling simulation process

Ball-end milling simulation operates step by step as it is depicted in Figure 2. Simulation's procedure steps are provided bellow:

1. Creation of solids: In this step, the user imports the appropriate geometrical data of the cutting tool and the workpiece. These parameters construct the three-dimensional solids of the cutter and the workpiece which are stored for later use.
2. Kinematics implementation: In this step, the cutting conditions are defined. The input parameters are related to the way of how the work piece surface is created. These parameters include axial and radial cutting depth, feedrate, inclination of cutting tool axis and discretization of tools' rotation.

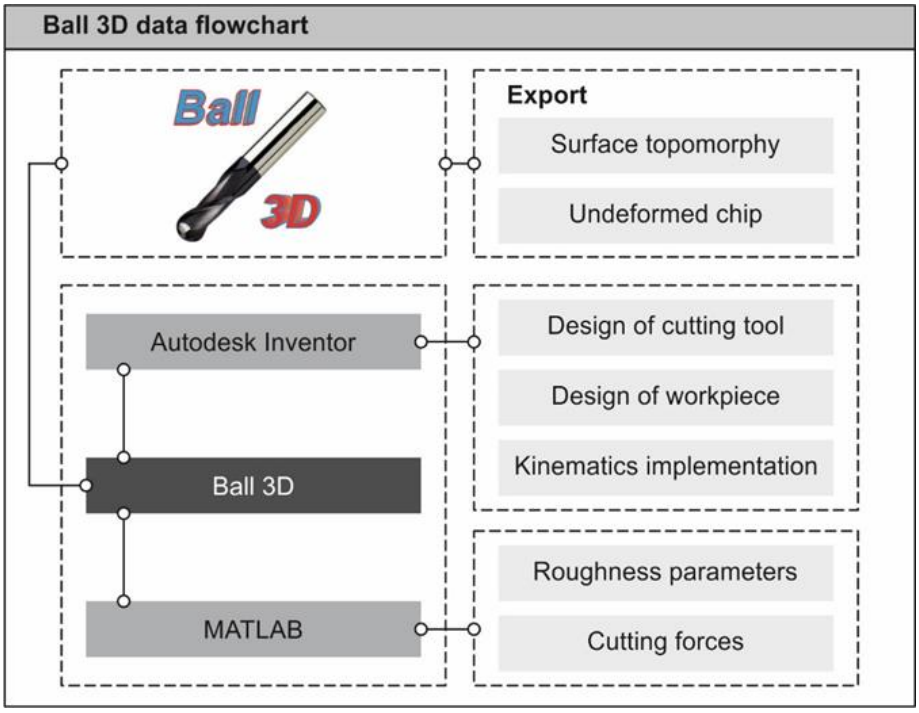

Fig. 1. Model data flowchart

3. Program execution: This step is performed simulation processing through successive placements of the cutting tool on the workpiece. The respective positioning in each step is based on the parameters set in the previous step.
4. Results export: In the end of the simulation process, the results are saved. The main results of the simulation are the resultant surface topomorphy and the representative undeformed chip of the cutting procedure at an intermediate position. Both of these results are stored in three-dimensional solid-form files.
5. Results post-processing: The final step is to analyze the topomorphy of the surface to be treated and the solid undeformed chip in order to estimate the surface roughness parameters and the cutting forces resulting respectively from the two solids.

2.3 Simulation model development

First of all, three dimensional objects of the cutting tool and the workpiece must be designed to simulate any ball-end milling procedure. The simulation stages, during model's execution are presented in Figure 3. Input data, required for models operation, are geometrical parameters of workpiece: length, width and height, cutting tool parameters: diameter, number of cuts and discretized rotation angle, and cutting conditions: feedrate, axial and radial depth of cut and inclination angle. All data above are key parameters, which define cutting tools' kinematics.

The next step is the creation of three dimensions solid models of workpiece and cutting tool. After kinematics definition, the process ends by sequentially repeating steps. When simulation is completed, two solid files have been produced. The first one is that of the machined workpiece and the other one is that of the undeformed chip.

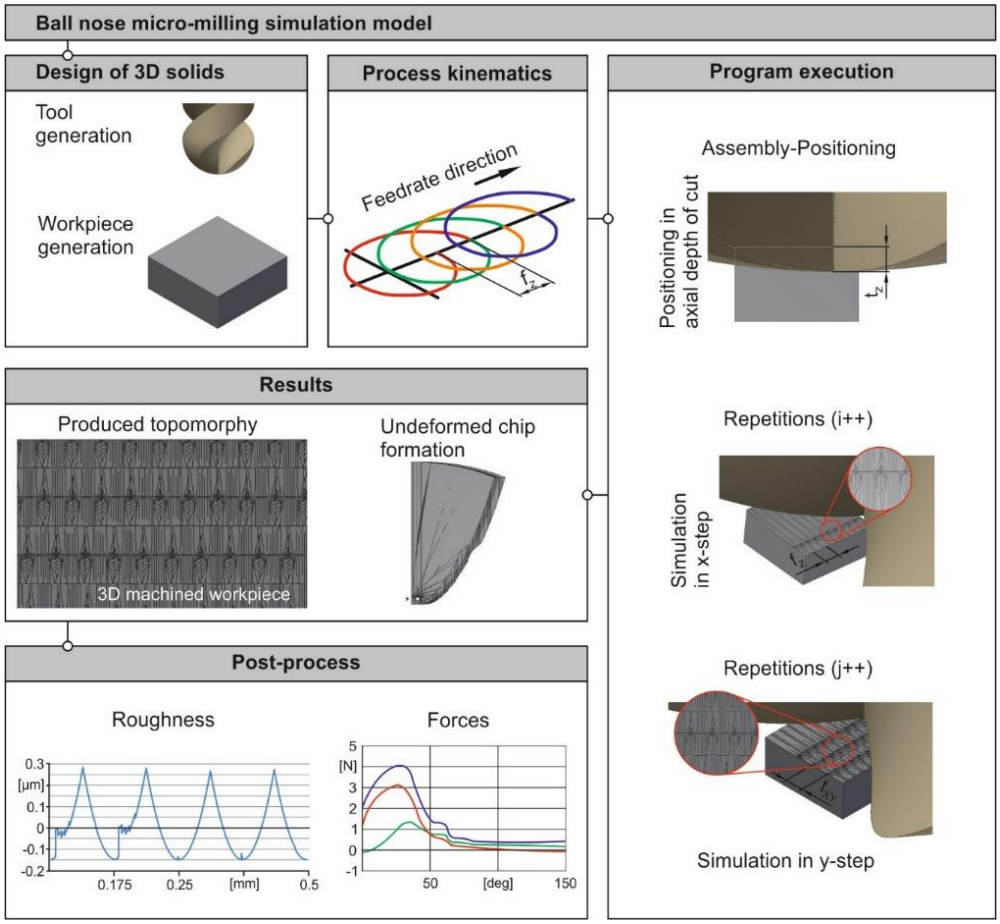

Fig. 2. Logic diagram: Basic simulation stages

The two three-dimensional results of the model contain the entire geometric information so that numerical characteristics results in measured by post-processing. Thus, the workpiece is used for the calculation of surface roughness, while the chip is used to calculate the cutting forces.

3. Parameters calculations and analysis

3.1 Surface roughness calculations

To calculate surface roughness, a code that would react on the produced surface of the simulation was developed. Initially, the finished workpiece is loaded. After determine the length of the workpiece and the number of roughness measurements onto the surface, the equal distances are calculated. Starting at the edge of the workpiece, a work plane is created on which, by the appropriate command, the cross-sectional points are plotted, as in Figure 4. Then, by assigning a distinct step, the coordinates of all the points on the two axes are obtained and stored in a text file of the .txt format. The points export process continues on the other levels that have been created.

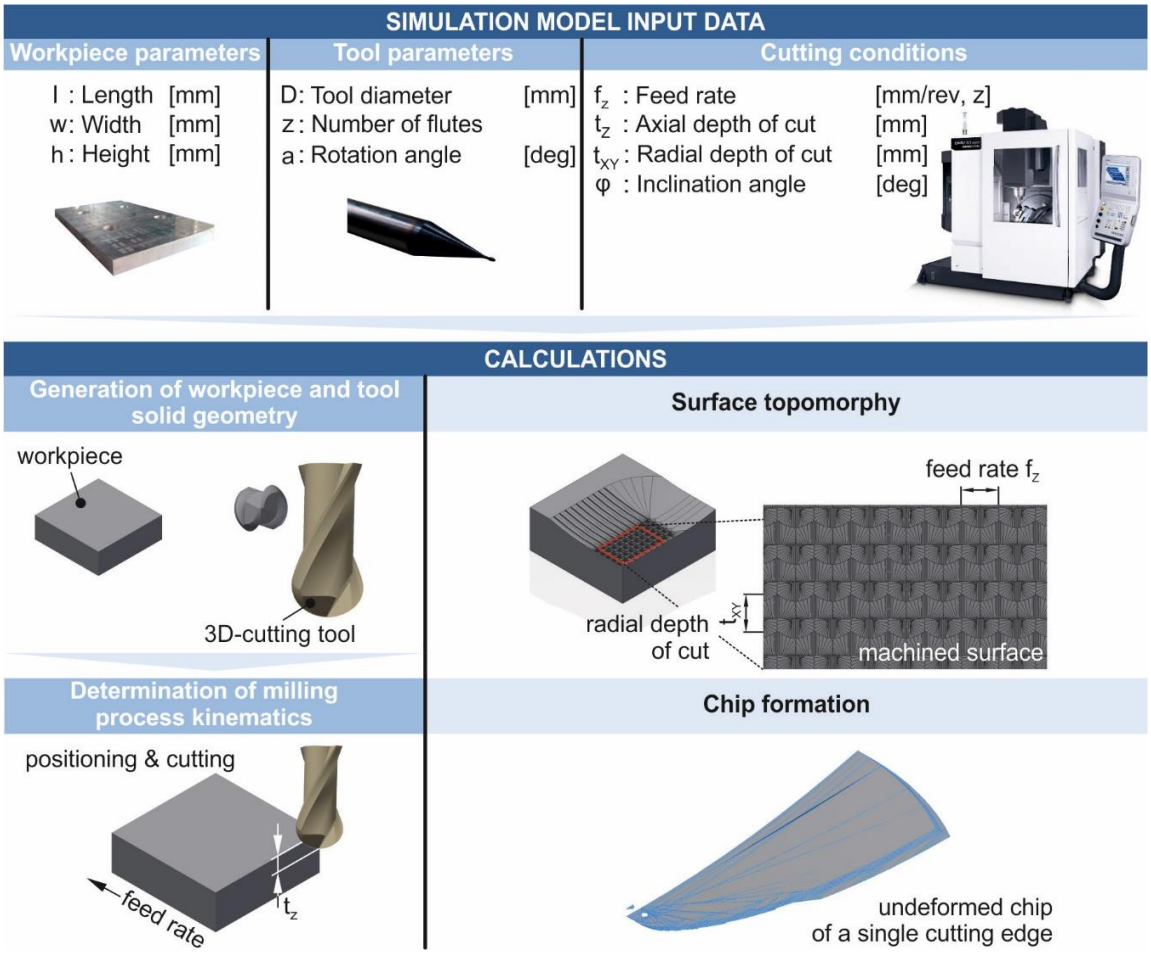

Fig. 3. Ball-end micro-milling simulation

Table 1 Main roughness parameters

Parameter	Nomenclature	Calculation type
Ra	Arithmetic average height	$Ra = 1n\Sigma\|yi\|ni=1$
Rz	Ten-point height	$Rz(ISO) = 1/n(\Sigma pi-\Sigma vini=1ni=1)$ $Rz(DIN) = 1/2n(\Sigma pi+\Sigma vini=1ni=1)$
Rt/Rmax	Maximum height of the profile	Rt = Rp + Rv

At first, there is the information of all points on each level. After removing the straight lines, the resulting curve is the waviness of the surface. For calculating the roughness curve, the average line is found as the average of all points. This line separates the curve into two spaces, the top and bottom, of the same area. The visualization of the mean line and the roughness curve are also graphical. The whole process is repeated for each separate level.

As having the roughness curve, it is now possible to determine the main roughness parameters (Ra, Rz, Rt) by applying the calculation types as shown in the following table (Gadelmawla *et al*. 2002).

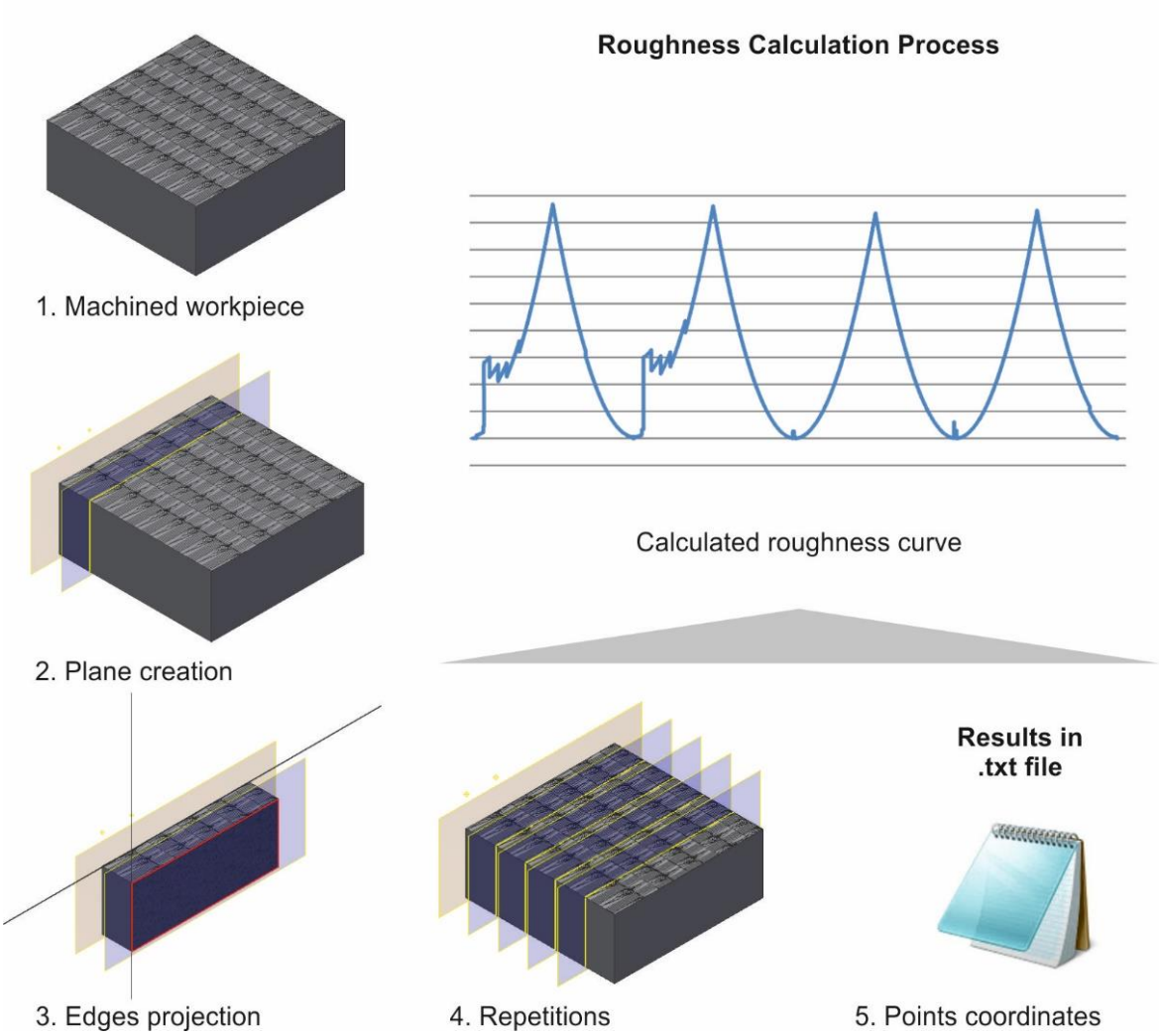

Fig. 4. Roughness calculation design

The arithmetic average height parameter Ra, also known as the centre line average (CLA), is an important parameter for general quality control. It is defined as the average absolute deviation of roughness irregularities from the mean line over one sampling length. The ten-point height parameter Rz, is more sensitive to occasional high peaks or deep valleys than Ra. It is defined as the average of summation of the five highest peaks and the five lowest valleys along the assessment length of the profile. Maximum height of the profile Rt, is very sensitive to the high peaks or deep scratches. It is defined as the vertical distance between the highest peak and the lowest valley along the assessment length of the profile. The three main parameters examined in this study are shown in the following Figure 5 (Gadelmawla *et al*. 2002).

Roughness parameters were calculated at specific distances on the cross-sectional planes of the workpiece (Figure 6). However, for calculating surface roughness parameters, the average of the values of the successive roughness measurements is used.

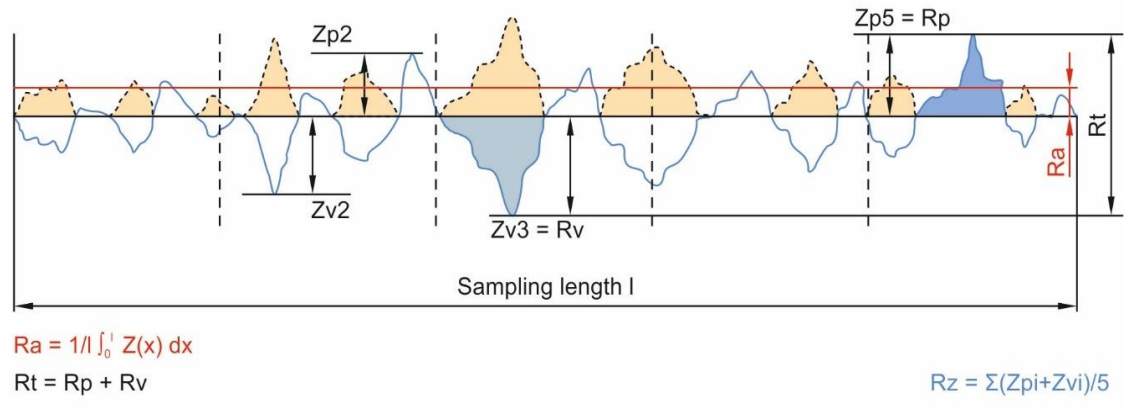

Fig. 5. Main roughness parameters

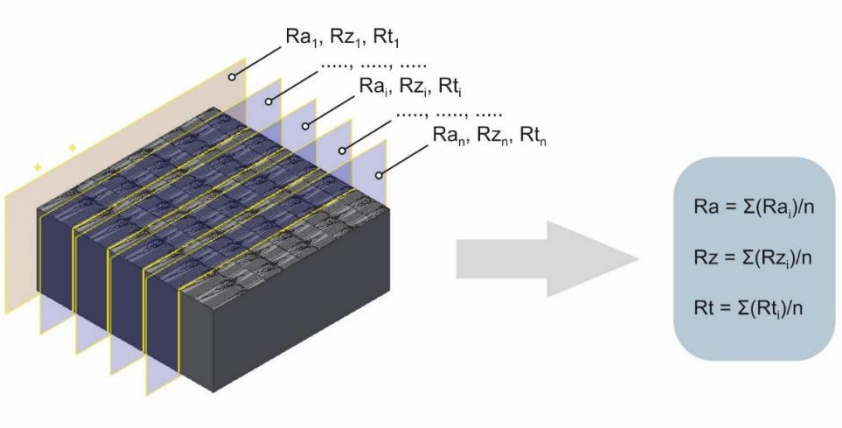

Fig. 6 Calculation of surface roughness parameters

3.2 Chip generation

The unformed chip is gradually made. To create a chip, a complete rotation of the cutter around its axis and a parallel displacement of its centre equal to the feedrate per revolution have to be applied. In this case, however, since the small-dimensional tool always has two principles, two identical chips are created. Thus, the representative undeformed chip is that one which is created by the tool 180° rotation and distance move equal to the half of the feedrate per revolution, that is equal to the feedrate per revolution and tooth.

The intersection of the tool with the workpiece is the elemental undeformed chip of each step. The assembly of all half-rotation elementary chips creates the representative undeformed of the machining process. The time and the steps required to create the chip depend on the discrete kinematic degree of the cutting tool that the user has defined before performing the simulation.

As the user has three-dimensionally stored the produced chip and the resultant machined surface implies that it carries all the geometric information of the machining, which may lead to subsequent processing of the results. Figure 7 shows 3D views of the assembled chip.

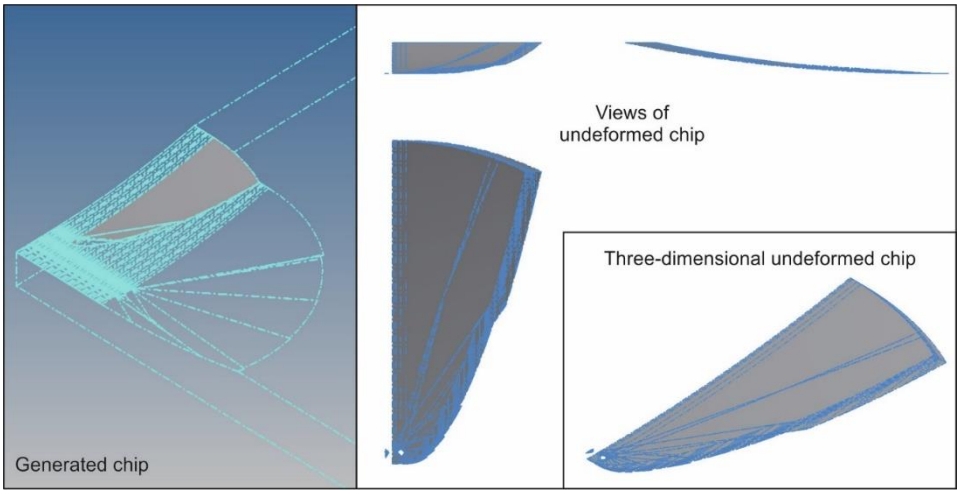

Fig. 7. Undeformed chip generation design

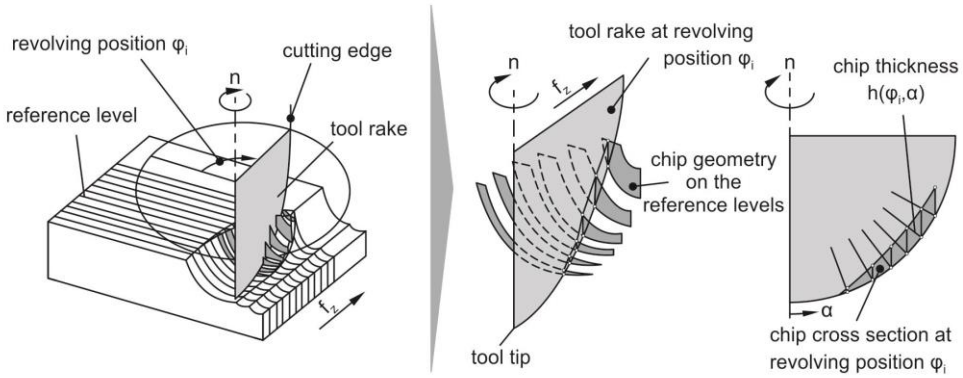

Fig. 8. Chip development process per rotation angle

3.3 Chip analysis – Cutting forces calculations

Cutting forces are calculated by processing the representative undeformed chip in an intermediate step of the simulation. The steps of the implemented algorithm are explained in detail below.

Initially, three-dimensional undeformed chip opens inside the CAD system. Vertical planes are then constructed at various angles of rotation, which divide the chip into sections. In the intersection of each plane with the chip, the specific geometry is displayed.

This surface is in the form of a meniscus part and constitutes the under consideration area of which the components of the cutting forces derive from in the specific rotation degrees (Figure 8).

This area is then divided into even smaller sections resulting from the line-radius design that have as origin the centre of the tool. Each straight line intersects the top and bottom surfaces of the chip forming quadrilaterals. Each tetrahedron is transformed into an approximate parallelogram by placing one side as the elementary width of the undeformed chip (bi) and the other as the average of the extreme values of the thickness of the chip (hi), as it is presented in Figure 9.

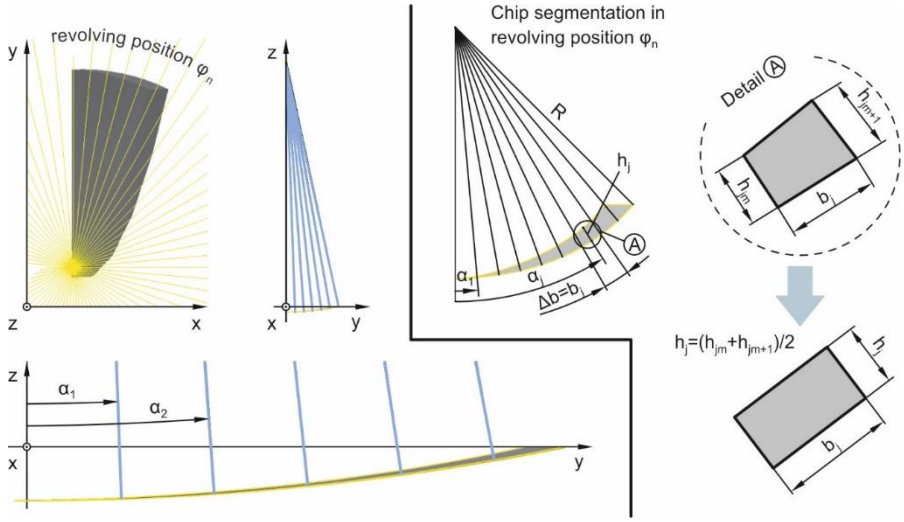

Fig. 9. Undeformed chip analysis

Using the geometric characteristics, width and thickness of the elementary undeformed chip, the three vertical force components Fci, Fti and Fni for the quadrangle are calculated according to the exponential equation of Kienzle and Victor. Based on this equation, the cutting forces depend exponentially on the thickness of the undeformed chip and linearly from its width. The three components of the cutting forces based on this model are given by the following relations (Kienzle, O. and Victor, H. 1957):

$$F_c = b \cdot k_{c1.1} \cdot h^{1-z} \tag{1}$$

$$F_t = b \cdot k_{t1.1} \cdot h^{1-y} \tag{2}$$

$$F_n = b \cdot k_{n1.1} \cdot h^{1-x} \tag{3}$$

Where:

Fc	cutting force component parallel to the cutting speed [N]
Ft	cutting force component parallel to the cutting edge [N]
Fn	cutting force component perpendicular to Fc and Ft [N]
b	chip width [mm]
h	chip thickness [mm]
kc1.1, kt1,1, kn1,1	cutting forces coefficients [N/mm^2]
z, x, y	material constants

Cutting force coefficients are defined as the force required for a cut of an undeformed chip with thickness and width equal to 1mm. Cutting force coefficients experimentally determined and altered according to the material, cutting edges of the cutting tool and cutting speed.

The total forces Fc, Ft and Fn for that particular rotational position are computed by vectorly summing the individual components. The transformation of forces to calculate the force components on the three main axes is done by applying the trigonometric relationships analyzed in the following Figure 10.

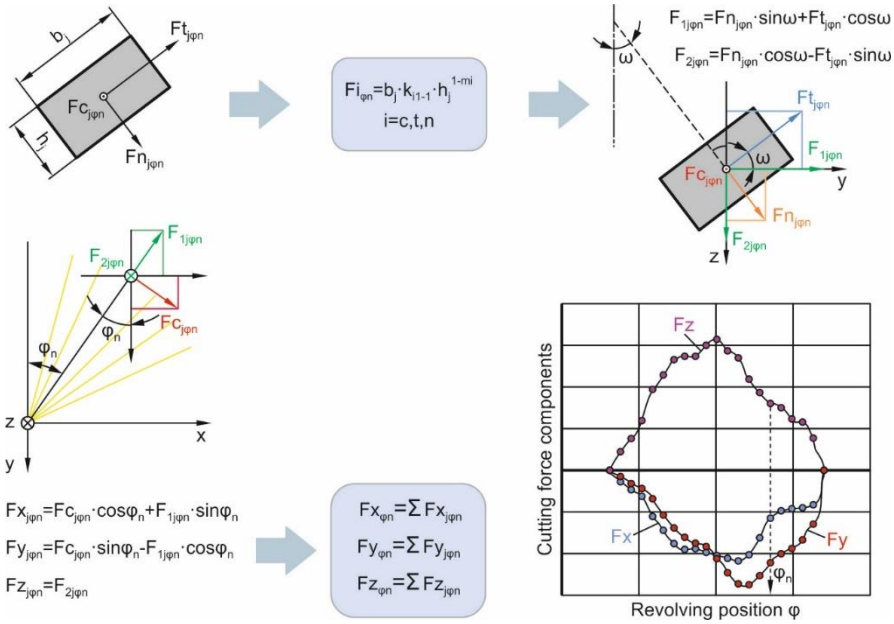

Fig. 10. Cutting forces calculation

From the analysis of the forces on the three axes for each part of the surface of the chip, the total forces of the three axes arise as sums. Since the calculation is made for each rotational position, it is easy to construct the rotation angle diagram with the constituent forces Fx, Fy and Fz.

The cutting force charts give a more direct view of their development during a complete rotation of the cutting tool and the maximum values of the components of each cutting force are easily distinguishable. At the same time, the evolution of the force is proportional to the geometry of the deceiver in a form similar to that projected within a dynamometer.

4. Material equipment and experimental procedure

A number of cutting experiments was carried out on a Deckel Maho DMU 50 eco milling machine, controlled by the Siemens control 810D. In order to confirm the simulation model and verify the results, cutting experiments with high-speed rotary chuck and tools with a diameter of less than 1 mm were performed at various cutting conditions. From the produced surfaces that emerged, the topomorphy was shown to vary according to the cutting conditions, the surface roughness and the cutting forces developed during the milling procedure were measured.

The material chosen for conducting the experiments is Al7075-T651. This material is widely used in the construction of structural components mainly in aeronautical applications. The aerospace industry requires materials that have high strength and as easy as possible machinability. The alloy Al7075 alloy heat treatment T651 combines high strength, medium hardness and corrosion resistance and is therefore preferred in the construction industry of structural components. Al7075 is an aluminum alloy with a primary zinc alloy element. It is a hard material with strength comparable to that of steel, with good fatigue strength and average workability but

Fig. 11. Experimental set up workflow

less corrosion resistance than other aluminum alloys. Its high cost limits its use only to applications where cheaper alloys are not suitable.

Cutting process was done in both vertical and tilted milling. Depending on the placement of the piece and the linear displacement of the tool, the cutting strategies were applied. When working with CNC machines, the exact measurement of the length and radius of the cutter is an important factor in the correct positioning of the cutting tools. The DMG Microset tool pre-setting device offers significant time and accuracy in tool readings and early identification of worn tools. The device works with the Microvision II IT software and features: Edge finder for fast cutting edge detection, robust die construction, pneumatic tightening on both axes, free moving linear guides and CMOS digital camera with telescopic lenses. The tool's radius and length values are entered into the machine's database so that the tool is ready for use.

To perform the experiments, a rotary high-speed micromilling chuck was used since the small diameter of the tools leads to high rotational speed values. IBAG HFK95 is specifically designed for machines with automatic tool change. It includes permanently self-lubricating roller bearings and it is cooled by compressed air. The rotation speed of the tool is adjusted by means of a rotary switch in the rotating inverter with which it is communicating.

The experiments were carried out in two main stages: Surface treatment experiments were initially carried out under various conditions and milling strategies, followed by experiments to control the cutting forces. The results were read using specialized equipment and software. Figure 11 shows the equipment used to prepare the experiments and analyze the results.

Aluminum alloy plate Al70175-T651 was used in the roughness experiments, where rectangular parallels of small and equal size 3x6 mm were cut. The size of the rectangle has been chosen so that a significant surface area is obtained to be measured in roughness, in stereoscopy and that does not take a long time to process. Each rectangle represents a specific data set of cutting conditions.

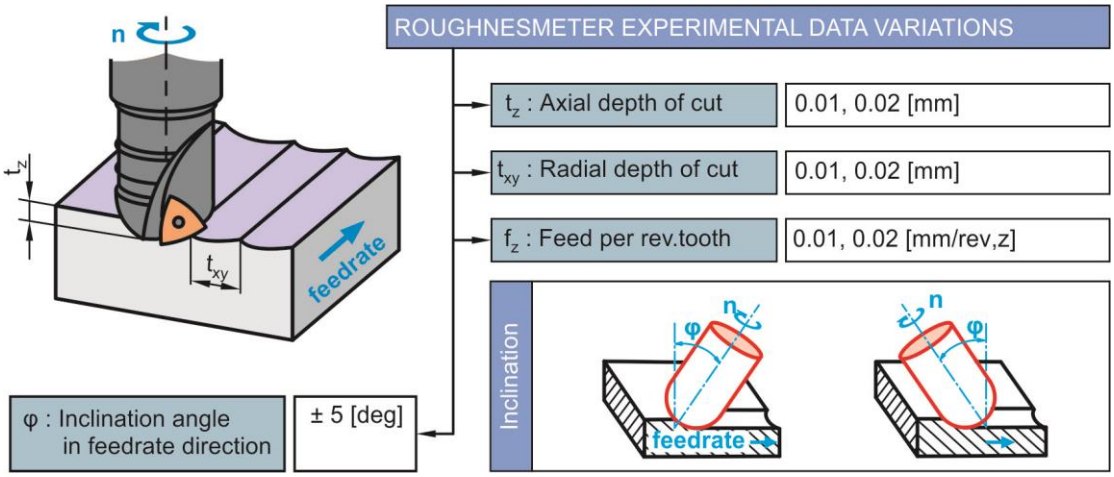

Fig. 12. Cutting conditions of roughness experiments

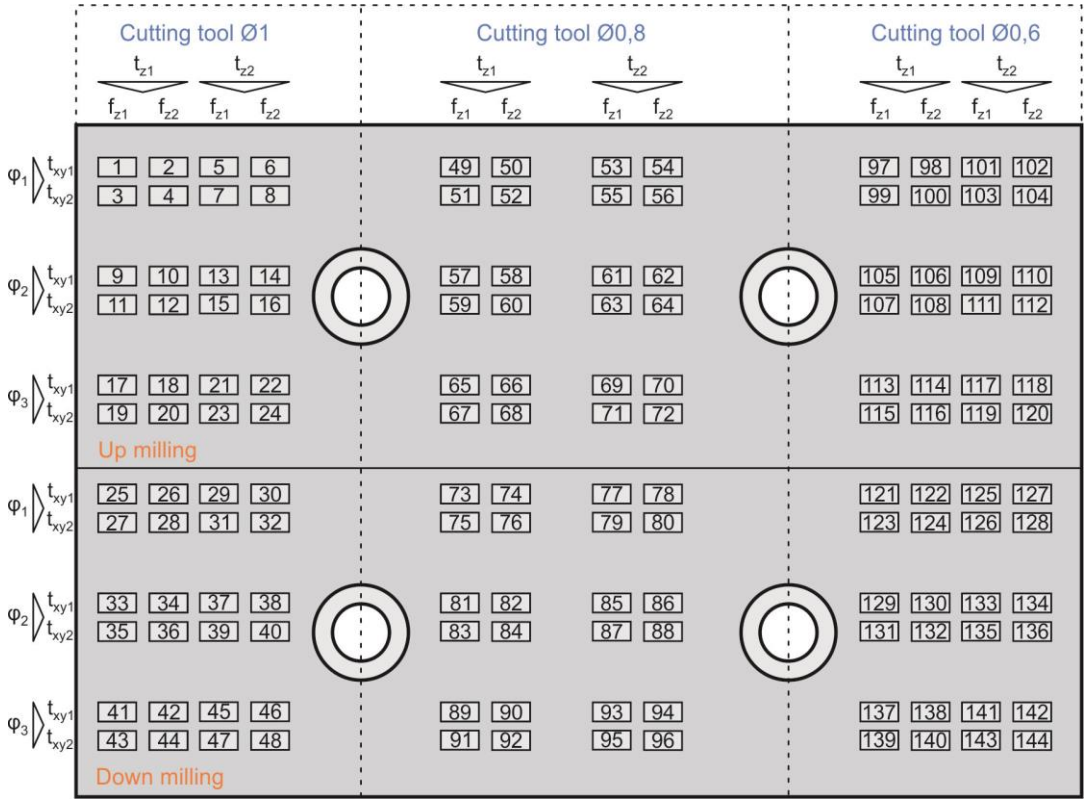

Fig. 13. Roughness experiments

For the verification of the model, three micro ball-milling tools of 1, 0.8 and 0.6 mm diameter were used. Three milling strategies of vertical, push milling 5 deg and pull milling 5 deg were used in both up milling and down milling. Axial and radial cutting depth values were 0.01 and 0.02 mm whereas feedrate values were 0.01 and 0.02 mm / rev, z. In the design of the experiments, the

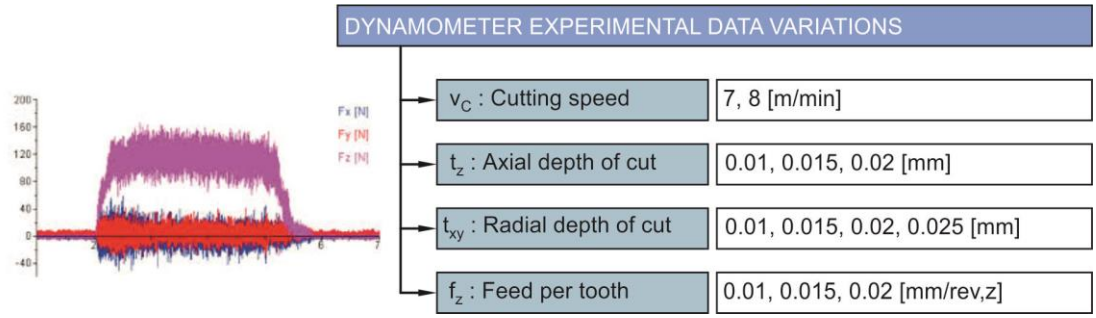

Fig. 14. Cutting conditions of cutting forces experiments

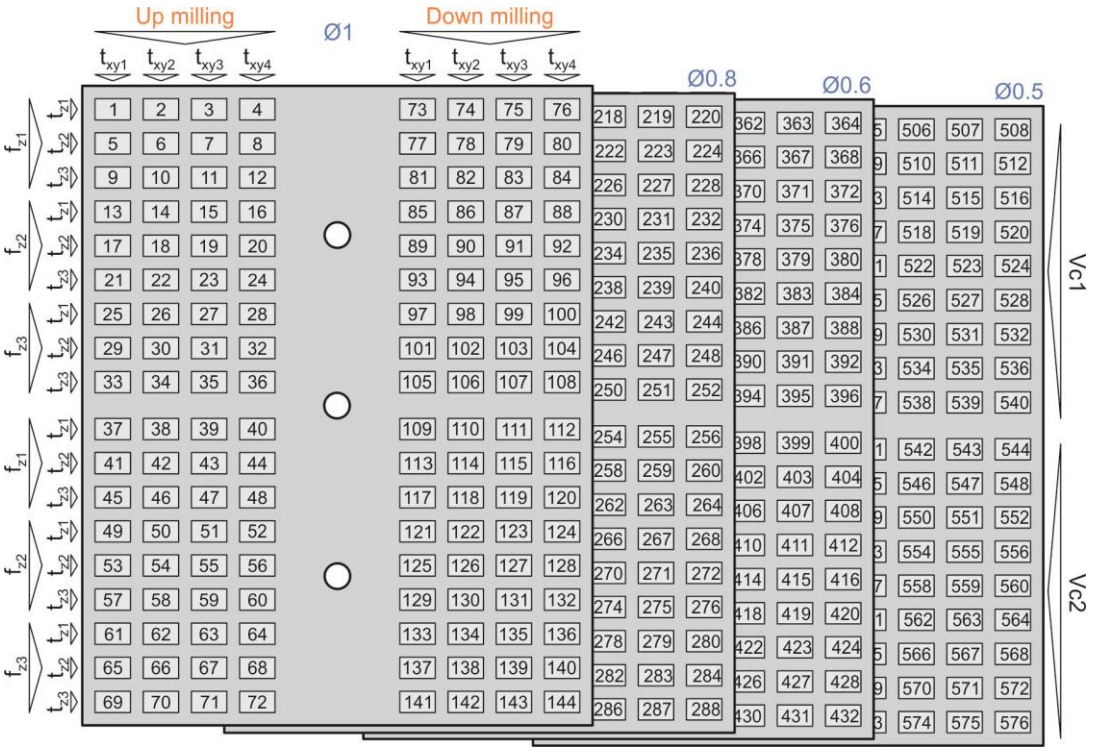

Fig. 15 Cutting forces experiments

complete factor was chosen so as to evaluate all interactions between the cutting conditions. The combination of these values results in 144 experiments.

The cutting conditions applied are summarized in Figure 12. The values of the conditions were based on the operating limits given by the manufacturer of the cutting tools while the rotational of the high-speed rotary chuck was determined based on the diameter of each cutting tool.

The placement of the experiments on the workpiece according to the cutting conditions and the cutting tool are shown in Figure 13.

Respectively, experiments were conducted to study the cutting forces. In these experiments it was not necessary to create a surface but to receive the signal of the forces on the three axes. In order to save time and wear the cutting tools and to ensure the correct measurement of the forces,

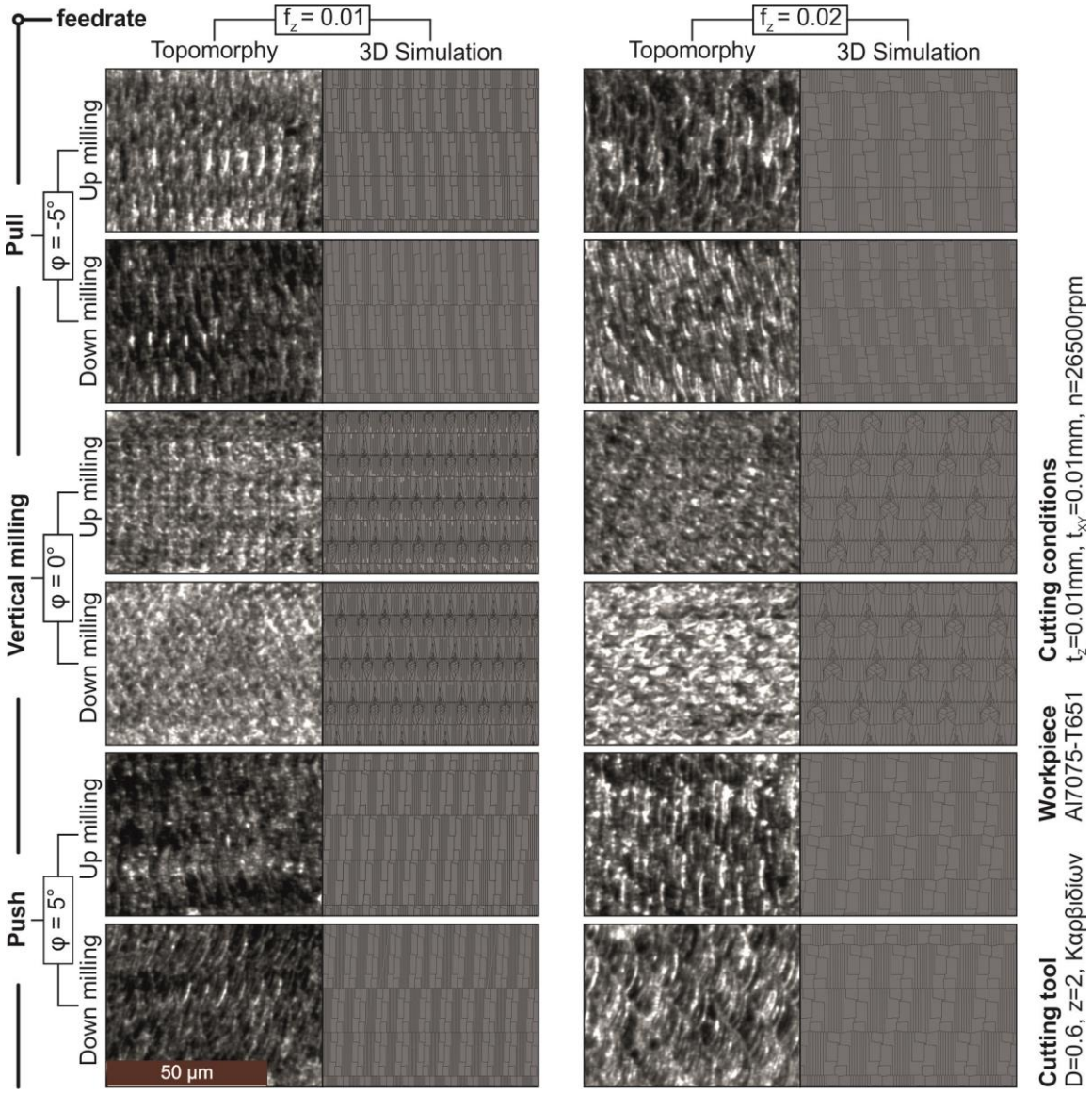

Fig. 16. Comparison of resulting 3D topomorphy with actual, Ø0.6mm

it was chosen to move the tool by three millimeters with respect to the direction of feedrate and three times the radial depth of cut.

To avoid vibrations within the measurements, small Al7075-T651 plates of 92 x 70 x 8 were used to fully sit on the micro-dynamometer and bolt them with screws. Based on the strength limits of the ball nose end mill given by the manufacturer, cutting conditions applied to the vertical cut. In particular, the conditions selected are those shown in Figure 14.

For each tool an Al7075-T651 aluminium plate was used. The design of the experiments is presented in the following Figure 15. A total of 576 separate dynamometers were developed.

5. Micromilling results and discussion

Experimental results were used to verify the simulation model.

5.1 Topomorphy results

Experiment stereoscopy revealed a first visual confirmation of the simulation model. The following Figure 16 shows the actual topomorphy in comparison with that of the three-dimensional simulation for specific cutting conditions. The comparison of the two topomorphies, real and simulated, in many cases, is easily perceived. The evaluation can be done using two main observations: By counting the passages that are shaped on both the horizontal and the vertical axis on a specific scale area and by a thorough focus on the resulting surface.

5.2 Surface roughness results

Using the stylus roughness meter and the optical profile meter, it was observed that the simulation model developed gave excellent results with a slight deviation from the actual values. Since the analysis of the values is made at the micrometer level, some deviations between the two instruments are expected. The reliability of the simulation model is evaluated based on the variations in roughness parameter values that it outputs as results with the values obtained from the two measuring instruments.

In most cases, the roughness values of the model are either between the corresponding values of the two measuring instruments or fairly close to them. This proves the verification of the model in Al7075-T651 alloy surface roughness prediction.

In the following Figure 17 the computational values of the model with the measured Rz experimental parameters for specific cutting conditions are presented for a 0.6 mm diameter ball nose end mill.

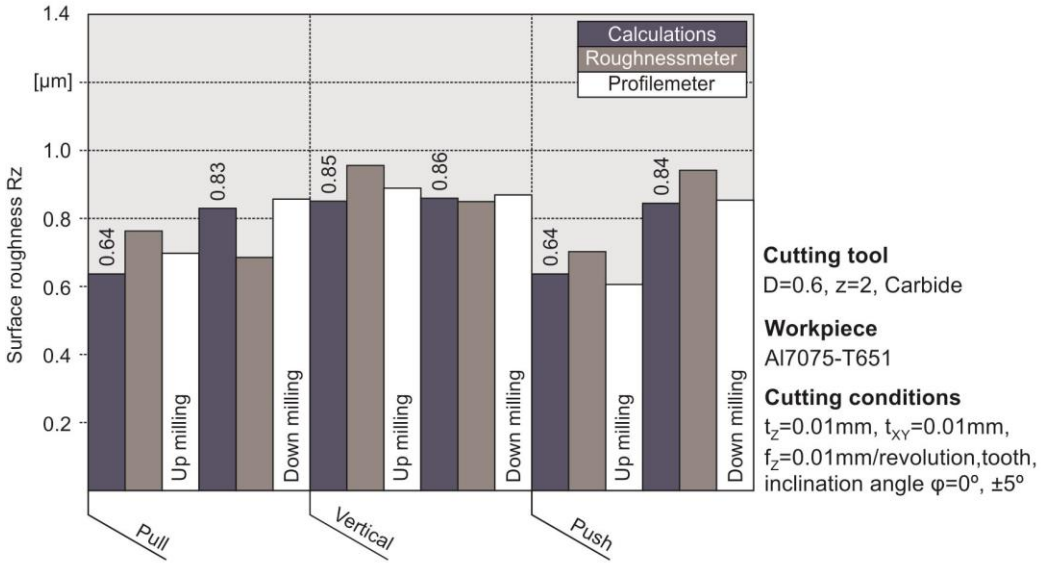

Fig. 17. Comparative roughness results Rz, Ø0.6mm

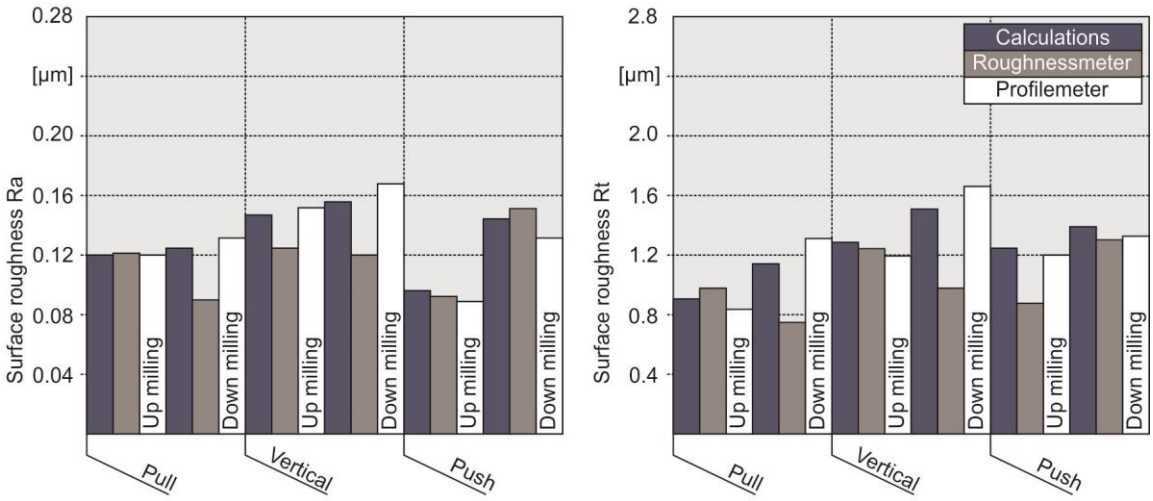

Fig. 18. Comparative roughness results Ra and Rt, Ø0.6mm

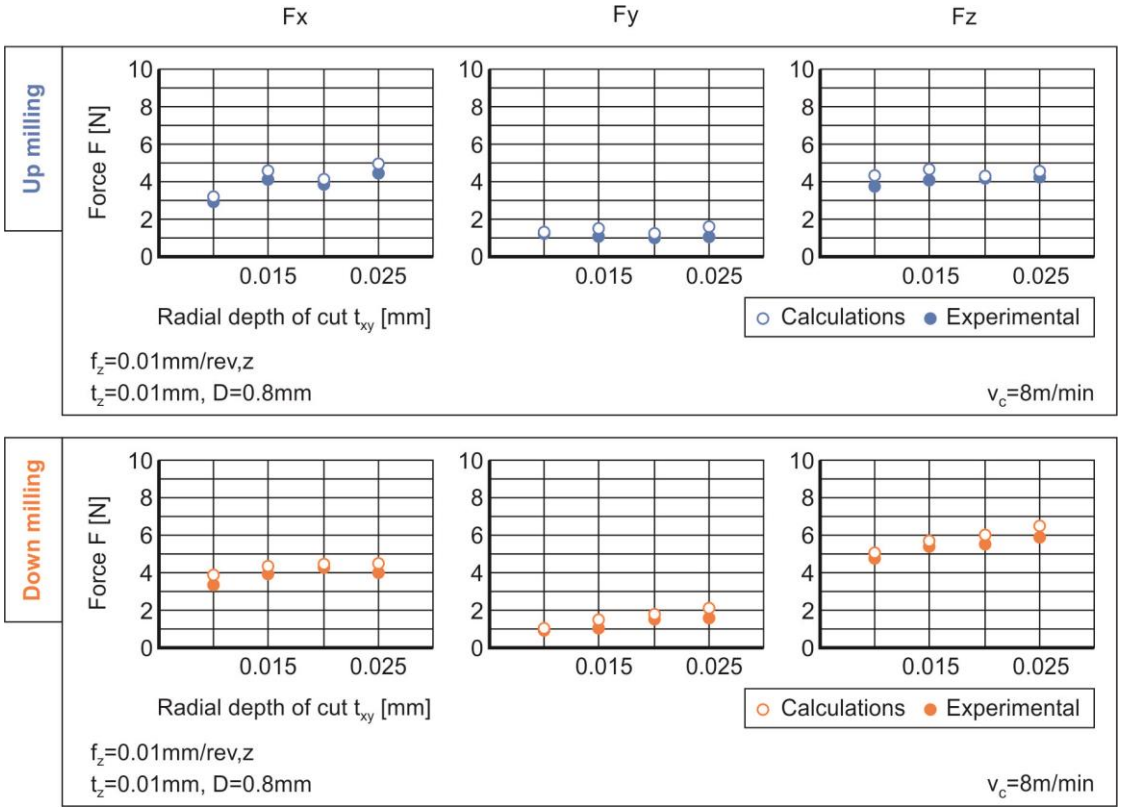

Fig. 19. Comparative results of maximum cutting forces, Ø0.8mm

Correspondingly, the diagrams of parameters Ra and Rt were constructed as shown in Figure 18. Obviously, as expected, the values of the Ra parameter are smaller than those of the Rz parameter and the larger values are those of the Rt parameter.

5.3 Cutting forces results

Similar to roughness, the comparison of cutting forces followed. Verification of the simulation model with respect to cutting forces is done through the experiments carried out on alloy plates Al7075-T651. Figure 19 below shows the experimental values of the maximum cutting forces compared to the theoretical values calculated from the simulation model for a 0.8 mm cutting tool with a cutting speed of 8 m/min, an axial cutting depth of 0.01 mm and a feedrate per revolution and tooth of 0.01mm / rev, z. According to the diagrams, the values of the cutting forces are approached to a large extent by the use of suitable coefficients, special cutting resistors and workpiece material constants.

6. Conclusions

In this work, the micromilling procedure was studied with a ball nose end-mill. This study was carried out in two stages: In the first stage, a simulation model of processing was developed based on a commercial CAD system and in the second stage verification and evaluation of experiments on Al7075-T651 were carried out. Evaluating the results of the simulation model, it is possible to draw useful conclusions regarding the reliability of the model.

By visual observation it is obvious that the results of the simulation model are verified to a great extent as there are similarities in the pattern of the surfaces. As a simulation, it was expected that the morphology of the produced surface could not be accurately mapped, as external factors such as the vibrations of the cutting tool were not included in the model but also because the cutting operation varies from machine tool to machine tool and from place to place even under the same cutting conditions.

Both roughness and cutting forces values calculated by the simulation model are very close to the experimental showing that a great reliability exists in all milling strategies for all the selected cutting conditions.

Acknowledgments

This research was supported by the Micromachining and Manufacturing Modeling Lab., School of Production Engineering and Management, Technical University of Crete.

References

Aurich, J.C., Bohley, M., Reichenbach, I.G. and Kirsch, B. (2017) “Surface quality in micro milling: Influences of spindle and cutting parameters”, *CIRP Annals*, **66**, 101-104. https://doi.org/10.1016/j.cirp.2017.04.029

Baburaj, M., Ghosh, A. and Shunmugam, M.S. (2017), “Study of micro ball end mill geometry and measurement of cutting edge radius”, *Precision Engineering*, **48**, 9-17. https://doi.org/10.1016/j.precisioneng.2016.10.008.

Baburaj, M., Ghosh, A. and Shunmugam, M.S. (2018), "Experimental and theoretical investigation on cutting forces in off-centre micro ball end milling", *CIRP J. Manufacture. Sci. Technol.*, **23**, 108-117. https://doi.org/10.1016/j.cirpj.2018.07.003

Cai, Y., Liu, Z., Shi, Z., Song, Q. and Wan, Y. (2016), "Influence of machined surface roughness on thrust performance of micro-nozzle manufactured by micro-milling", *Exp. Thermal Fluid Sci.*, **77**, 295-305. https://doi.org/10.1016/j.expthermflusci.2016.05.004

Chen, N., Chen, M., Wu, C. and Pei, X. (2017), "Cutting surface quality analysis in micro ball end-milling of KDP crystal considering size effect and minimum undeformed chip thickness", *Precision Eng.*, **50**, 410-420. https://doi.org/10.1016/j.precisioneng.2017.06.015

Chen, W., Huo, D., Teng, X. and Sun, Y. (2017), "Surface Generation Modelling for Micro end Milling Considering the Minimum Chip Thickness and Tool Runout", *Procedia CIRP 2017*, **58**, 364-369. https://doi.org/10.1016/j.procir.2017.03.237

Chen, W., Zheng, L., Xie, W., Yang, K. and Huo, D. (2019), "Modelling and experimental investigation on textured surface generation in vibration-assisted micro-milling", *J. Mater. Process Technol.*, **266**, 339-350. https://doi.org/10.1016/j.jmatprotec.2018.11.011

Eifler, M., Klauer, K., Kirsch, B., Seewig, J. and Aurich, J. C. (2018), "Micro-milling of areal material measures – influences on the resulting surface topography", *Procedia CIRP*, **71**, 122-127. https://doi.org/10.1016/j.procir.2018.05.083

Gadelmawla, E. S., Koura, M. M., Maksoud T. M. A., Elewa I. M. and Soliman H. H. (2002), "Rougness parameters", *J. Mater. Process Technol.*, **123**, 133-145.

Kienzle, O. and Victor, H. (1957). "Spezifische schnittkräfte bei der metallbearbeitung", *Werkstattstechnik und Maschinenbau*, **47**, 224-225.

Kuram, E. and Ozcelik, B. (2013), "Multi-objective optimization using Taguchi based grey relational analysis for micro-milling of Al 7075 material with ball nose end mill", *Measurement*, **46**(6), 1849-1864. https://doi.org/10.1016/j.measurement.2013.02.002.

Liu, Q., Cheng, J., Xiao, Y., Yang, H. and Chen, M. (2018) "Effect of milling modes on surface integrity of KDP crystal processed by micro ball-end milling", *Procedia CIRP*, **71**, 260-266. https://doi.org/10.1016/j.procir.2018.05.060

Luo, S., Jun, M. B. and Dong, Z. (2016), "Numerical simulation of chip ploughing volume and forces in 5-axis CNC micro-milling using flat-end mills", *Procedia Manufacturing*, **5**, 348-361. https://doi.org/10.1016/j.promfg.2016.08.030

Pratap, T. and Patra, K. (2018), "Fabrication of micro-textured surfaces using ball-end micromilling for wettability enhancement of Ti-6Al-4V", *J. Mater. Process Technol.*, **262**, 168-181. https://doi.org/10.1016/j.jmatprotec.2018.06.035

Vehmeyer, J., Piotrowska-Kurczewski, I., Böhmermann, F., Riemer, O. and Maaß, P. (2015), "Least-squares based parameter identification for a function-related surface optimisation in micro ball-end milling", *Procedia CIRP*, **31**, 276-281. https://doi.org/10.1016/j.procir.2015.03.076

Vyboishchik, A. V. (2016), "Modelling topology of freeform surfaces with ball-end milling", *Procedia Engineering*, **150**, 761-767. https://doi.org/10.1016/j.proeng.2016.07.103

Wang, Y., Zou, B., Wang, Z., Huang, C. and Liu, Z. (2018), "Analyzing the performance of self-developed cermet micro end mills in machining of TC4 alloy micro-grooves", *Procedia CIRP*, **71**, 424-428. https://doi.org/10.1016/j.procir.2018.05.056

Wojciechowski, S., Maruda, R. W., Krolczyk, G. M. and Niesłony, P. (2018), "Application of signal to noise ratio and grey relational analysis to minimize forces and vibrations during precise ball end milling", *Precision Eng.*, **51**, 582-596. https://doi.org/10.1016/j.precisioneng.2017.10.014

Wojciechowski, S., Wiackiewicz, M. and Krolczyk, G.M. (2018), "Study on metrological relations between instant tool displacements and surface roughness during precise ball end milling", *Measurement*, **129**, 686-694. https://doi.org/10.1016/j.measurement.2018.07.058

Wojciechowski, S.; Mrozek, K. (2017) "Mechanical and technological aspects of micro ball end milling with various tool inclinations", *J. Mech. Sci.*, **134**, 424-435. https://doi.org/10.1016/j.ijmecsci.2017.10.032

Xie, J., Li, Y. H. and Yang, L. F. (2015), "Study on 5-axial milling on microstructured freeform surface using

the macro-ball cutter patterned with micro-cutting-edge array", *CIRP Annals*, **64**(1), 101-104. https://doi.org/10.1016/j.cirp.2015.04.075.

Zhang, X., Zhang, J., Zheng, X., Pang, B. and Zhao, W. (2017), "Tool orientation optimization of 5-axis ball-end milling based on an accurate cutter/workpiece engagement model", *CIRP J. Manufacture. Sci. Technol.*, **19**, 106-116. https://doi.org/10.1016/j.cirpj.2017.06.003

CC